ELSEVIER

Journal of Alloys and Compounds 265 (1998) 264–268

Journal of ALLOYS AND COMPOUNDS

Influence of amorphization on electrode performances of AB_2 type hydrogen storage alloys

Xiaoguang Yang[a,*], Yongquan Lei[a], Chunsheng Wang[b], Guangming Zhu[a], Wenkui Zhang[a], Qidong Wang[a]

[a]*Department of Materials Science and Engineering, Zhejiang University, Hangzhou 310027, China*
[b]*Department of Physics, Zhejiang University, Hangzhou 310027, China*

Received 25 April 1997; received in revised form 31 May 1997

Abstract

It is generally accepted that the electrochemical discharge capacity of a hydrogen storage alloy is closely related to its crystal characteristics. From our experiment, the discharge capacity of AB_2 type Laves phase hydrogen storage alloy $ZrCr_{0.4}Mn_{0.2}V_{0.1}Ni_{1.3}$ decreased sharply from 324 mAh g^{-1} to 25 mAh g^{-1} after amorphization by mechanically milling the crystalline (as-cast) alloy with stainless steel balls. We believe that for the as-cast alloy, hydrogen atoms stored in the tetrahedral interstitial sites of Zr_2B_2 (B=Cr, V or Ni) all contribute to its electrochemical capacity. However for the amorphous alloy only hydrogen atoms in low-energy Zr_3B and Zr_4 tetrahedral interstitial sites contribute to its electrochemical capacity. We also believe that only half of the total sites in the crystalline or amorphous alloys can absorb and desorb hydrogen atoms reversibly, and that the process of ball milling manages to lower the barrier potential for the hydrogen discharge reaction by about 60 kJ (mol H)$^{-1}$. We resolve the phenomenon into the finer particles including abundant hydrogen diffusion channels and the formation of a looser tetrahedral interstitial structure in the metal glass. © 1998 Elsevier Science S.A.

Keywords: Zr-based hydrogen storage alloy; Crystal characteristics; Electrochemical capacity

1. Introduction

AB_2 hydrogen storage alloys are promising for negative electrodes in nickel–metal hydride batteries for their higher discharge capacities and better resistance to oxidation than those of AB_5 alloy [1,2]. As AB_2 type multiple-phase hydrogen storage alloys are mainly composed of C14, C15 Laves phase, and some solid solutions with bcc structure [3], there exist abundant boundaries, with enriched electrochemically catalytic elements as active reaction sites and diffusion pipes for transporting reactants and products. Hout and coworkers [4,5] investigated the relationship amongst the crystal structure, phase abundance and electrode performance of (Zr, A) $V_{0.5}Ni_{1.1}Mn_{0.2}Fe_{0.2}$ (A=Ti, Nb or Hf) and found that the alloy with the C15 phase displayed a large reduction in discharge capacity when the discharge current was increased, but that alloys composed only of the C14 phase showed better high-rate dischargeability.

Recently we studied the dependence of the electrochemical properties of $Zr(Cr_xNi_{1-x})_2$ ($0.15 \le x \le 0.65$) hydrogen storage alloys on the composition and crystalline characteristics [6,7]. It was found that the main crystal structure of $Zr(Cr_xNi_{1-x})_2$ alloys changed from C15 to C14 at $x=0.45$~0.50, and that the C15 alloy $Zr(Cr_{0.35}Ni_{0.65})_2$ had a maximum electrochemical discharge capacity of 305 mAh·g^{-1} and excellent electrochemical cycling stability at ambient temperature. Also Yu [8] examined the as-cast $ZrMn_{0.6}Cr_{0.25}Ni_{1.3}$ alloy with the Rietveld refinement method and confirmed that the alloy consisted of C15 as its main phase, along with small amount of C14, Zr_7Ni_{10} and Zr_9Ni_{11}. After the alloy annealing at 1333 K for 8 h, the Zr_7Ni_{10} phase disappeared, and the structure of its C15 main phase tended to be more stable because of the good arrangement of A atoms in the space lattice, which incurred a deterioration of the electrochemical discharge capacity.

In the present paper, we have studied the influence of amorphization on the electrochemical capacity of $ZrCr_{0.4}Mn_{0.2}V_{0.1}Ni_{1.3}$ alloy in comparison with that of a

*Corresponding author.

0925-8388/98/$19.00
PII S0925-8388(97)00287-9

crystalline alloy of the same composition, and tried to explain the differences in electrochemical properties.

2. Experiment details

The ingots of $ZrCr_{0.4}Mn_{0.2}V_{0.1}Ni_{1.3}$ alloy were prepared by arc-melting under Ar atmosphere and were remelted 3 times to ensure homogeneity. The as-cast alloy ingots were mechanically crushed to particles of about 300 mesh for XRD analysis and for test electrode preparation as described previously [6]. For XRD analyses, a Rigaku C-max-III B diffractometer with Cu Kα radiation and a nickel diffracted-beam filter was used.

Ball milling on the above alloy powder was performed in a planetary mill; the alloy powder and hardened steel balls in a weight ratio of 1:15 were put into tubs under an Ar atmosphere at 1 bar. The mill worked for 30 min and rested for 30 min periodically. The total work time was up to 70 h or 85 h (the last 15 h without rest).

The hydride electrodes were prepared by cold pressing the mixtures of different alloy powder and powdered electrolytic copper (300 mesh) in the weight ratio of 1:2 into copper holders to form porous pellets of 10 mm in diameter. Electrochemical charge–discharge tests were carried out in a standard open trielectrode electrolysis cell, in which nickel oxyhydroxide was used as the counter-electrode, Hg/HgO was used as the reference electrode and 6M KOH solution was used as electrolyte. The discharge capacities of hydride electrodes were determined by a galvanostatic charge–discharge method. The electrodes were fully charged at a current density of 100 mA g^{-1} and discharged at 50 mA g^{-1} to the cut-off potential set at -0.6 V.

3. Results and discussion

Fig. 1(A), (B) and (C) are the XRD patterns of the hydrogen storage alloy $ZrCr_{0.4}Mn_{0.2}V_{0.1}Ni_{1.3}$ in different states. Fig. 1(A) shows the diffraction pattern of as-cast alloy, whose main phase is the fcc C15 Laves phase structure with a crystal parameter (a)=0.7062 nm, while the extra peaks on 2θ=37.8° and 40.23° belong to orthorhombic Zr_7Ni_{10} and tetragonal Zr_9Ni_{11} phases, respectively. It was found that the main part of the milled alloy powder lost their crystalline character owing to partial amorphization after 70 h ball-milling, while a small part of alloy still remained in the C15 phase structure with its distorted lattice, since there is a obvious shift in the d values of their Braggs peaks. Amorphization was completed when a more continuous 15 h milling was added.

Fig. 2 shows the variations of electrochemical discharge capacities of hydrogen storage alloys $ZrCr_{0.4}Mn_{0.2}V_{0.1}Ni_{1.3}$ in the as-cast state, after 70 h and 85 h milling with cyclings. The as-cast alloy has no electrochemical

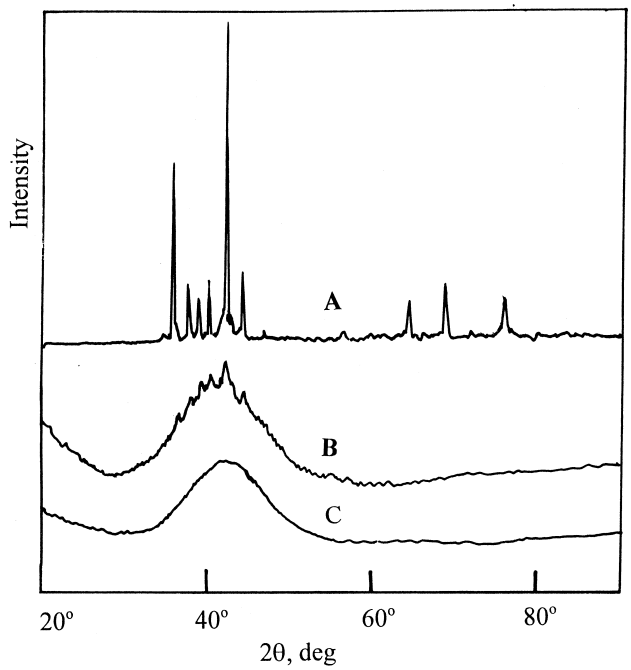

Fig. 1. XRD of $ZrCr_{0.4}Mn_{0.2}V_{0.1}Ni_{1.3}$ hydrogen storage alloys. A: as-cast, B: milled for 70 h, C: milled for 85 h.

discharge capacity in the first 3 cycles and reaches its maximum of 324 mAh g^{-1} after 14 cycles; However, the alloy milled for 70 h is able to discharge a capacity of 21 mAh g^{-1} which is 60% of its maximum (i.e. 35 mAh g^{-1} at a discharge current density of 50 mA g^{-1} and mild temperature) at the first cycle, and the charge–discharge cycle number for reaching its maximum discharge capacity is only 3. A similar tendency exists for the corresponding amorphous alloy which has an even smaller maximum discharge capacity (25 mAh g^{-1}). We conclude that the ball-milling is able to shorten the activation cycle number noticeably. By SEM analyses, lots of inside cracks were found in the bulk alloy powder.

Fig. 3 shows the anodic polarization curves of the above three kinds of electrodes in their activated condition. There is no apparent discharge potential plateau for the ball-milled electrodes. Their discharge capacities are much less than that in as-cast state. We believe that for the discharge capacity 35 mAh g^{-1} of the 70 h milling electrode, there is a contribution from the part alloy remaining in the crystalline state. The amorphization milling severely deteriorates the charge–discharge property of the alloy $ZrCr_{0.4}Mn_{0.2}V_{0.1}Ni_{1.3}$.

The reason for the sharp decrease in discharge capacity is that the C15 Laves phase structure of the alloy has vanished.

Each unit cell of the AB_2 type Laves phase consists of 2 A atoms and 4 M or Ni atoms, and contains 1 M_4, 4 AM_3 and 12 A_2M_2 tetrahedral interstitial sites (TISs). The number of the different tetrahedral interstitial sites in the cell of the hydrogen storage alloy $ZrM_{0.7}Ni_{1.3}$ ($M_{0.7}$=

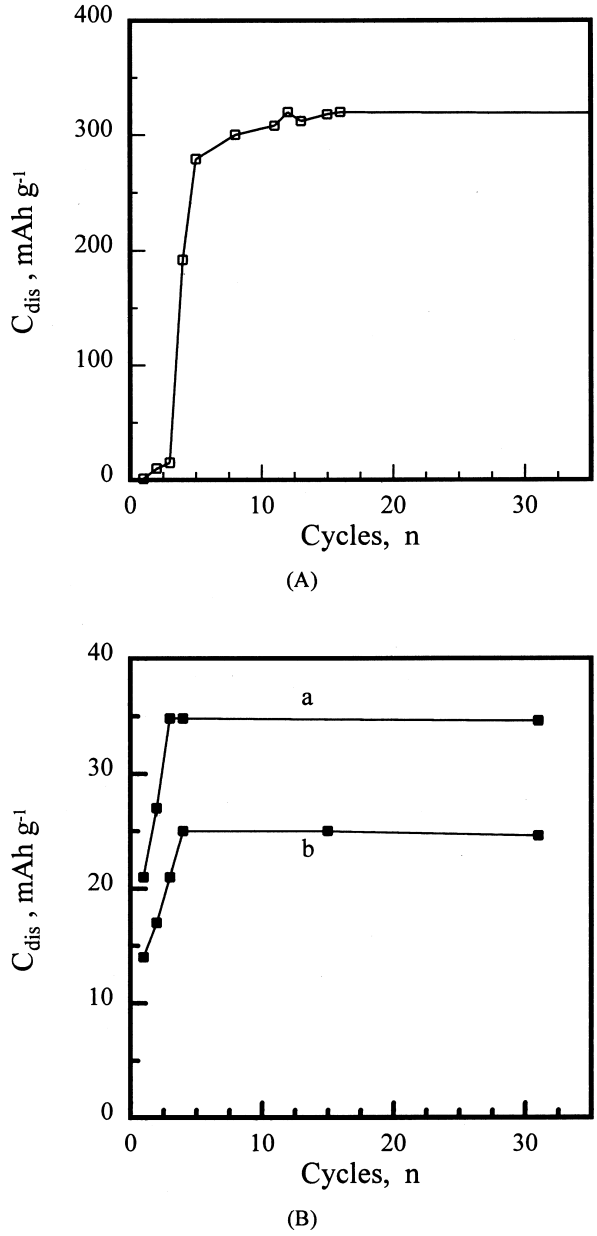

Fig. 2. (A) The variation of electrochemical capacity of the as-cast $ZrCr_{0.4}Mn_{0.2}V_{0.1}Ni_{1.3}$ with cyclings. (B) The variation of electrochemical capacity of the milled $ZrCr_{0.4}Mn_{0.2}V_{0.1}Ni_{1.3}$ with cyclings. a: milled for 70 h, b: milled for 85 h.

$Cr_{0.4}Mn_{0.2}V_{0.1}$) is listed in Table 1. It is naturally accepted that the M_4 or ANi_3 site can not accommodate hydrogen atoms stably in the test condition.

The electronic static repulsive force makes the tetrahedral interstitial sites which share a common triangle face unable to absorb hydrogen atoms at the same time. This means that only half of the $Zr_2(M, Ni)_2$ type interstitials listed in Table 1 can reversibly absorb/desorb hydrogen atoms. According to a previous study [9], AB_2 type Zr-based Laves phase alloy is multiphase, and its C15 main phase is 65 wt.% only and a small amount of C14 can reversibly absorb–desorb hydrogen. On this basis the

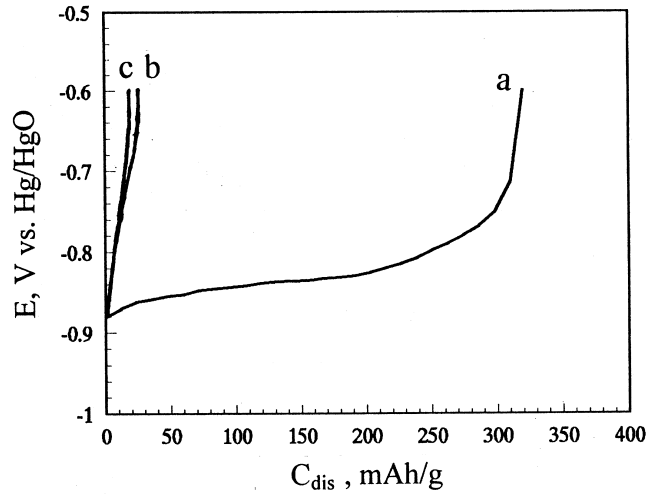

Fig. 3. The anodic polarization curves of $ZrCr_{0.4}Mn_{0.2}V_{0.1}Ni_{1.3}$ hydride electrodes. A: as-cast, B: milled for 70 h, C: milled for 85 h.

calculated discharge capacity is about 321.2 mAh g^{-1}, which is close to the measured value (324 mAh g^{-1}, discharge to −0.6 V cut-off potential at a current of 50 mA g^{-1} and 298 K).

However, hydrogen atoms probably also occupy the tetrahedral interstitial sites $A_{4-n}B_n$ (n=0, 1, 2, 3, 4) in the amorphous alloy $A_{1-x}B_x$ (i.e. $Zr_{1-x}Ni_x$) combining with Early transition metal and Late transition metals (ETM–LTM), the maximum of hydrogen absorbing capacity in each type interstitial site can be obtained by the following equation [10]:

$$C_{n,\max} = \frac{1.9 \times 4!}{n!(4-n)!} x^n (1-x)^{4-n} \quad (1)$$

where $C_{n,\max}$ is the hydrogen storage capacity (H/metal atom) of $A_{4-n}B_n$ TIS, and x is the concentration of the B atom (Ni or M).

Ciureanu et al. also have reported that several new anodic maxima have been observed in cyclic voltammograms after long-term cycling and attributed this to the oxidation of hydrogen atoms stored in low-energy TISs, such as Zr_4 and Zr_3Ni [11]. Accordingly the amorphous alloy $ZrCr_{0.4}Mn_{0.2}V_{0.1}Ni_{1.3}$ can be rewritten as $Zr_{0.33}B_{0.67}$ (B=Cr, Mn, V or Ni). Table 2 also lists the calculated and measured electrochemical discharge capacities contributed by Zr_3B and Zr_4 which are two types of tetrahedral interstitial sites. It was found that only half of the Zr_3B and Zr_4 tetrahedral interstitial sites can reversibly electrochemically charge/discharge as the corresponding alloy in the as-cast state does. The calculated discharge capacity is 26.96 mAh g^{-1} which is in good agreement with the measured value of 25.0 mAh g^{-1}.

The atomic disorder surrounding the interstitial sites leads to the variation in chemical potentials of hydrogen atoms in the same type interstitial holes, and to the difference in electrode potential as well, and then the

Table 1
The number of tetrahedral interstitial sites (TISs) per unit cell and the calculated and measured electrochemical discharge capacity of $ZrM_{0.7}Ni_{1.3}$ ($M_{0.7}=Cr_{0.4}Mn_{0.2}V_{0.1}$) hydrogen storage alloy (mAh g^{-1}), 298 K

Type of TIS	$(M, Ni)_4$	$Zr(M, Ni)_3$				$Zr_2(M, Ni)_2$		
		$ZrNi_3$	$ZrMNi_2$	ZrM_2Ni	ZrM_3	Zr_2M_2	Zr_2MNi	Zr_2Ni_2
Number of TIS/cell	1	0.95	0.93	2.03	0.09	1.22	5.96	4.82
Total number of TIS/cell	1	4				12		
Calculated C_{dis}	–	–	30.55	66.65	2.955	40.05	195.8	156.4
Total Calculated C_{dis}	–	100.2				392.3		
Measured C_{dis}		324						

Table 2
The maximum of the hydrogen storage capacities in Zr_3B and Zr_4 holes and the calculated and measured electrochemical discharge capacity of amorphous $Zr_{0.33}B_{0.67}$ (B=Cr, Mn, V, Ni) hydrogen storage alloy (mAh g^{-1}), 298 K

Type of TIS	Zr_4	Zr_3B
$C_{n\ max}$ (H/M atom)	0.0225	0.183
$C_{n\ dis}$ (mAh g^{-1})	5.92	48.0
Calculated C_{dis}	26.96	
Measured C_{dis}	25.0	

amorphous electrode exhibits a smooth electrochemically discharging curve as shown in Fig. 3.

We also try to analyze the results from the enthalpy change of the hydriding process. The enthalpy E_n of hydrogen in the tetrahedral interstices $A_{4-n}B_n$ of hydrogen storage alloys can be calculated with a weighted ratio according to that of the imaginary hydrides (AH_2, BH) as in [12]:

$$E_n = \frac{[(4-n)H_0(AH_2) + nH_0(BH)]}{4} \quad (2)$$

Table 3 lists the calculated enthalpies E_n of hydrogen in different $A_{4-n}B_n$ TISs. There are many more differences among the four type sites. For the as cast (crystalline) alloy, hydrogen atoms stored in A_2B_2 with a suitable chemical potential level, mainly contribute to the electrochemical discharge capacity at room temperature; while for the amorphous alloy with the same chemical composition, hydrogen atoms restored in sites with a lower theoretical energy potential (i.e. A_4 and A_3B) bring forth the reversible discharge capacity. The difference implies that the metal glass stored extra energy during the amorphization process by ball-milling. Because of the reoccurrence of discharge capacity and an anodic polarization curve, the induced extra energy does not release during charging/discharging process.

Table 3
The enthalpy E_n of different tetrahedral interstitial sites $A_{4-n}B_n$ in the $Zr_{0.33}B_{0.67}$ hydrogen storage alloy, kJ (mol H^{-1}) (B=Cr, Mn, V or Ni)

TIS	A_4	A_3B	A_2B_2	AB_3
E_n	−164	−117~−131	−73~−92	−28~−53

The enthalpy E_n of hydrogen in the fourfold coordinated interstitial sites of A_2B_2 and AB_3 in the C15 phase structure, which is determined by the weighted average theoretical enthalpies of imaginary binary hydrides, is regarded as approximating to the real potential for the electrochemically discharging hydrogen, that is, the potential energy for discharging hydrogen is within −28~−92 kJ (mol H)$^{-1}$. The result is in agreement with −38~−100 kJ (mol H)$^{-1}$ concluded by Harris according to Nerst's law [10].

As we know, the lower energy sites, Zr_4 and Zr_3Ni in the metal glass, take part in absorbing/desorbing hydrogen reaction, but their calculated site energies (−117~−164 kJ (mol H)$^{-1}$) are more negative than the real reaction energy with a disparity of about −60 kJ (mol H)$^{-1}$.

The amorphization process makes the crystal alloy fracture to a smaller particle size, and destroys the long range atomic order spacing to turn it into a chemically random state. It was found that the distances of Ni–Ni and La–Ni pairs in the amorphous film $LaNi_5$ prepared by sputtering were larger than those of crystalline $LaNi_5$ alloy [13]. So the fourfold coordinated interstitial sites have a looser structure than the compacted ones in crystalline alloy. Hydrogen atoms manage to enter or to leave the TISs more easily in the transition metal glass bulk. Smaller alloy particle sizes and a larger hydrogen diffusion coefficient also make the glass electrode activation easier. Otherwise, the hydrogen diffusion is restrained in the initial activating cycles because of the perfect crystalline structure and longer hydrogen diffusion distances for the as-cast alloys. When the hydrogen diffusion pipes, such as microcracks and permeable surfaces, are established, and the diffusion distance is reduced due to the particle pulverization by hydrogen-induced expansion, the activation process is completed.

4. Conclusion

There is a close relationship between the Laves phase structure and the electrochemical discharge capacity of hydrogen storage alloy $ZrCr_{0.4}Mn_{0.2}V_{0.1}Ni_{1.3}$ or $Zr_{0.33}B_{0.67}$ (B=Cr, Mn, V or Ni). It is mainly half of the Zr_2B_2 TISs in the as-cast alloy that contributes to the electrochemical

discharge capacity at room temperature. After the amorphization process by ball-milling, the corresponding alloy has a sharp decrease in capacity, and half TISs of Zr_3B and Zr_4 can provide reversible capacity as well. Extra energy of about 60 kJ (mol H)$^{-1}$ induced during the milling process can lower the potential of the electrochemically discharging hydrogen reaction.

Acknowledgements

Financial support by Chinese National ‘‘863’’ Program and National Natural Science Foundation of China and technical assistance by Prof. G.L. Lu and Dr. W.H. Liu are gratefully acknowledged.

References

[1] S.R. Ovshinsky, M.A. Fetcenko, J. Ross. Science 260(9) (1993) 176.
[2] H. Sawa, S. Wakao, Mater. Trans. JIM 31(6) (1990) 487.
[3] H. Iba, E. Akiba, J. Japan Inst. Metals 59(4) (1995) 456.
[4] J. Huot, E. Akiba, T. Osura, Denki Kagaku 61(12) (1992) 1424.
[5] J. Hout, E. Akiba, T. Osura, Y. Ishido, J. Alloys Comp. 218 (1995) 101.
[6] Y.Q. Lei, X.G. Yang, Q.D. Wang, J. Wu, J. Alloys Comp. 231 (1995) 573.
[7] X.G. Yang, Y.Q. Lei, Q.D. Wang, J. Wu, Trans. Nonferrous Met. Soc. China 5 (1995) 61.
[8] J.Y. Yu, Y.Q. Lei, C.P. Chen, Q.D. Wang, J. Alloys Comp. 231 (1995) 574.
[9] Y.Q. Lei, J.Y. Yu, X.G. Yang, Q.D. Wang, G.L. Lu, Acta Metall. in Sinica (in Chinese) 32(7) (1996) 779.
[10] J.H. Harris, W.A. Curtin, M.A. Tenhover, Phy. Rev. B 36(11) (1987) 5784.
[11] M. Ciureanu, D.H. Ryan, J.O. Ström-Olsem, M.L. Trudeau, J. Electrochem. Soc. 140(3) (1993) 579.
[12] P.S. Rudman, G.D. Sandrock, Ann. Rev. Mater. Sci. 12 (1982) 271.
[13] H. Sakaguchi, S. Tomoyoshi, K. Moriuchi, G. Adachi, Int. Symp. on Metal–Hydrogen Sys., Fundamentals and Applications, Japan, Tokyo, Nov 6–11, 1994.